

Received December 24, 2020, accepted January 12, 2021, date of publication January 19, 2021, date of current version January 27, 2021.

Digital Object Identifier 10.1109/ACCESS.2021.3052893

# Local Carpet Bombardment of Immobilized Cancer Cells With Hydrodynamic Cavitation

MOEIN TALEBIAN GEVARI<sup>1,2,3</sup>, GIZEM AYDEMIR<sup>4,5</sup>, GHAZALEH GHARIB<sup>2,3</sup>,  
OZLEM KUTLU<sup>2</sup>, HUSEYIN UVET<sup>5</sup>, MORTEZA GHORBANI<sup>3,6,7</sup>, AND ALI KOŞAR<sup>1,2,7</sup>

<sup>1</sup>The Ångström Laboratory, Division of Solid State Electronics, Department of Electrical Engineering, Uppsala University, 75237 Uppsala, Sweden

<sup>2</sup>Faculty of Engineering and Natural Science, Sabanci University, 34956 Istanbul, Turkey

<sup>3</sup>Nanotechnology Research and Application Center, Sabanci University, 34956 Istanbul, Turkey

<sup>4</sup>The Institute for Intelligent Systems and Robotics (ISIR), Sorbonne University, 75005 Paris, France

<sup>5</sup>Department of Mechatronics Engineering, Yildiz Technical University, 34349 Istanbul, Turkey

<sup>6</sup>Department of Biomedical Engineering and Health Systems, KTH Royal Institute of Technology, SE-141 57 Stockholm, Sweden

<sup>7</sup>Center of Excellence for Functional Surfaces and Interfaces for Nano-Diagnostics (EFSUN), Sabanci University, 34956 Istanbul, Turkey

Corresponding authors: Morteza Ghorbani (mortezag@kth.se) and Ali Koşar (kosara@sabanciuniv.edu)

This work was supported in part by the TUBITAK (The Scientific and Technological Research Council of Turkey) Support Program for Scientific and Technological Research Project under Grant 217M869 and Grant 118S040, and in part by the Sabanci University Internal Project under Grant I.A.CF-18-01877.

**ABSTRACT** This study presents a method based on carpet bombardment of immobilized cells with cavitating flows. For this, immobilized cancer cell lines are exposed to micro scale cavitating flows from the tip of a micro nozzle under the effect of cavitation microbubbles. The deformation as a result of cavitation bubbles on exposed cells differs from one cell type to another. Therefore, the difference in cell deformation upon cavitation exposure (carpet bombardment) acts as a valuable indicator for cancer diagnosis. The developed system is tested on HCT-116 (Human Colorectal Carcinoma), MDA-MB-231 (Breast Adenocarcinoma), ONCO-DG-1 (Ovarian Adenocarcinoma) cell lines due to their clinical importance. The mechanical effects of cavitation are examined by considering the single-cell lysis effect (the cell membrane is ruptured, and the cell is destroyed) with the help of the Scanning Electron Microscopy (SEM) technique. Our study proposes a promising label-free method for the potential use in cancer diagnosis with cavitation bubble collapse, where microbubbles could be precisely controlled and directed to the desired locations, as well as the characterization of the biophysical properties of cancer cells. The proposed approach tool has the advantages of label-free approach, simple structure and low cost and is a substantial alternative for the existing tools.

**INDEX TERMS** Cancer diagnosis, hydrodynamic cavitation, spray structure, cavitation bubble, cancer cells.

## I. INTRODUCTION

According to the thermodynamic phase diagram, either an increase in the temperature or a decrease in the static pressure of the liquid leads to liquid-gas phase change [1]. Hydrodynamic cavitation originating from the decrease in the static pressure results in the nucleation of microbubbles. Depending on the system geometry and working principle, it generates a high amount of energy upon the collapse of emerging bubbles [2]. Due to a wide variety of potential cavitation applications, many researchers have conducted studies on the cavitation physics to facilitate earlier inception [3], [4] and to intensify cavitating flows [5]. The energy released from the collapse of cavitation bubbles has been effectively employed for various applications such as wastewater treatment [6], food manufacturing [7], energy harvesting [8], [9],

bacterial inactivation [10], biomedical treatment [11], and other industrial applications [12].

The use of hydrodynamic cavitation in biomedical applications is an emerging field in the literature. Cavitation implementation in biological systems offers many lanes and possibilities in diagnosis and therapy. Cavitation effects on tissues and cells [13]–[15] have been well recognized to play an instrumental role in biomedical applications such as blood-brain barrier opening with the use of focused ultrasound [16], shock wave lithotripsy [17], histotripsy [18], sonoporation [19], laser surgery [20], characterization [21], [22], and manipulation of single cells techniques [23]. For example, Miller *et al.* [14] studied physical and chemical mechanisms of inertial cavitation, which appeared to be promising in causing ultrasonic effects on cells, which were investigated by changing the quantity and environment of the cells. Recent research has shown that high focal pressure could mechanically erode soft tissues as a result of the

The associate editor coordinating the review of this manuscript and approving it for publication was Gustavo Callico<sup>1</sup>.

nonlinear effects created by cavitation. The tissue fragmentation method, which has been used in kidney stone treatment, involves liquefying the tissue rather than thermally destroying it [24]. Therefore, the mentioned cavitation-based techniques have been proven as therapeutic methods on various diseases, such as the prostate diseases [24], hepatocellular carcinoma (HCC) [25] and deep vein thrombosis (DVT) [26].

To use hydrodynamic cavitation in various biological applications such as cancer therapy and the mechanical effects of hydrodynamic cavitation on both cancer cells and healthy tissues should be investigated. Thus, by examining the impact of hydrodynamic cavitation on a single cell, its local effects on cells and tissues could be revealed, which will pave the way to all potential therapeutic and diagnostic applications as well as drug treatments.

This study aims to investigate the effects of hydrodynamic cavitation on immobilized single cancer cells. This work involves a label-free technique, which can disrupt the cancer cell cytoplasmic membrane pores and its granular surface structure using hydrodynamic cavitation. The cavitation phenomenon is also characterized before the experiments on cells inside the microchannel with an inner diameter of 256  $\mu\text{m}$ . The spray structure under the effect of hydrodynamic cavitation at different inlet pressures is studied and analyzed accordingly. By evaluating the energy released from the collapse of the cavitation bubbles within the spray structure, we demonstrate that our approach represents a unique technique on both cancer and endothelial cells without any prior chemical treatment, which might affect the cell membrane properties substantially. The ability of cancer cells to occupy, starting from the basement membrane, is defined as a critical step during metastasis. The basal membrane disruption causes changes in cancer cells' cytoskeleton architecture and the mechanical flexibility. Hence, it is a promising method for the characterization of the biophysical properties of cancer cells, which are known to be stiffer than their healthy counterparts. The developed system is tested on HCT-116 (Human Colorectal Carcinoma), MDA-MB-231 (Breast Adenocarcinoma), ONCO-DG-1 (Ovarian Adenocarcinoma) cell lines due to their clinical importance. The mechanical effects of cavitation are examined by considering the single-cell lysis effect (the cell membrane is ruptured, and the cell is destroyed) with the help of the Scanning Electron Microscopy (SEM) technique.

In the following sections, first, cavitating flows are characterized with water as the working fluid, and the results are compared with the case of PBS. Thereafter, the results of cell experiments on cavitating flow characterization and on different cancer cells are presented. This study aims to propose an innovative concept for a cancer diagnostic platform to the interdisciplinary research community.

## II. MATERIALS AND METHODS

The spray structure under the effect of hydrodynamic cavitation was analyzed at different upstream pressures with both water and 1xPBS as the working fluids. For this, the

hydrodynamic cavitation test rig was assembled and the cavitating flow was exposed to the targeted cells according to the optimized upstream pressures.

### A. THE EXPERIMENTAL SETUP AND PROCEDURE

The experimental setup in this study consists of a fluid container (Swagelok, Erbusco BS, Italy) connected to a high-pressure pure nitrogen tank (Linde Gas, Gebze, Kocaeli, Turkey), which pushes the working fluid through the stainless-steel tubing of the experimental setup (See Supplementary Information 3, Figure S4). In order to obtain the required pressure drop to initiate the hydrodynamic cavitation, a polyether ether ketone (PEEK) microtube with an inner diameter of 256  $\mu\text{m}$  was used as the constriction element. Omega pressure gauge was also used to measure the pressure of the working fluid at the inlet of the PEEK tube. A T-type filter (Swagelok) capable of particle removal with a nominal size of 15  $\mu\text{m}$  was also used to remove the unwanted particles in the working fluid. The sample was placed on a transparent holder 15 mm away from the tip of the nozzle during the experiments. All the equipment in touch with the biological samples was sterilized prior to the experiments with 70% ethanol. The working fluid (to generate the spray under the effect of hydrodynamic cavitation) was the commercial sterile PBS. A high-speed camera with proper lightening system was used to monitor and analyze the fluid flow patterns for the fluidic section of this study. In order to make flow characterization in this study, a transparent ruler is installed on the experimental setup to facilitate the jet separation distance measurement. For this section, the backpressure was increased gradually, and the flow patterns were monitored at different pressures. Each experiment was repeated for 3 times to check for the repeatability. An SEM sample preparation protocol (See Supplementary Information 4) was performed on the samples, and further assessment about cell morphology (including size and shape before and after the cavitation exposure) was provided by the Scanning Electron Microscopy (SEM, Zeiss Leo Supra 35 VP, Germany) technique at an acceleration voltage of 2 kV. Figure S6 shows the schematic of the experimental setup and procedure in this study.

PBS was used to preserve the viability of the cells to some extent. Another countermeasure taken for this purpose was to keep the cells in the culturing medium throughout the experiment process except for the short time (3 seconds) of the cavitation exposure. Furthermore, the experimental setup was sterilized regularly. Cells were cultured (See Supplementary Information 5) on a 5  $\text{cm}^2$  silicon wafer surface with a density of  $1 \times 10^4$  cells/ $\text{cm}^2$ . 0.5 mL culture medium was added for each square centimeter of culture vessel growth surface area.

## III. RESULTS

### A. SPRAY UNDER THE EFFECT OF CAVITATION

There are different non-dimensional numbers in the literature, which were presented in order to study the stability of liquid jet flows. Reynolds number [27], which is the ratio between inertial forces and viscous forces, is used to characterize

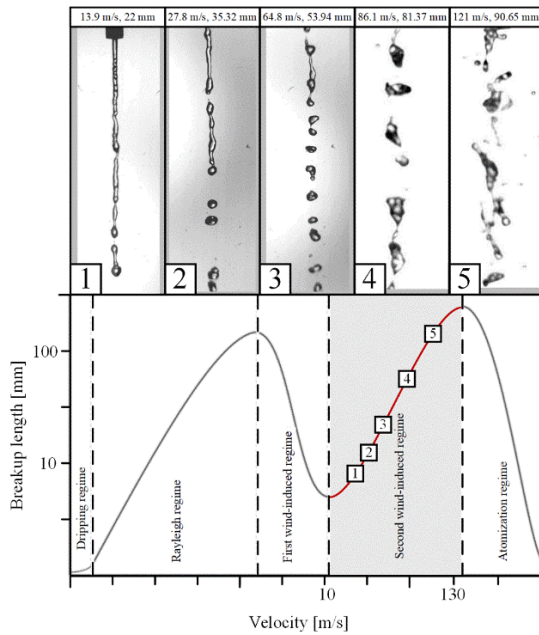


FIGURE 1. Spray flow regime and separation length for water as the working fluid.

the fluid flow:

$$Re = \frac{\rho u L}{\mu} \quad (1)$$

where  $\rho$  is the density of the working fluid,  $u$  is the average velocity,  $L$  is the length scale, and  $\mu$  is the viscosity of the working fluid.

Weber number [27], which stands for the ratio between kinetic energy and surface energy, is defined as:

$$We = \frac{\rho r u^2}{\gamma} \quad (2)$$

where  $r$  is the radius of the water cylinder from the nozzle and  $\gamma$  is the surface tension of the working fluid. Weber number displays the tendency of the liquid jet to break-up.

Ohnesorge number [28] is used to show the effect of viscosity on the jet behavior:

$$Oh = v \sqrt{\rho/h\gamma} \quad (3)$$

where  $v$  is the kinematic viscosity of the working fluid.

Figure 1 demonstrates the relationship between the flow velocity and break-up length for different flow regimes. The backflow pressure is increased gradually, and the spray is visualized at 70, 345, 690, 1380, and 2070 kPa. The velocity is calculated from mass flow rate measurements. The jet velocity at different upstream pressures ranged roughly between 13 m/s to 120 m/s.

The separation length from the tip of the nozzle increases with the flow velocity. This suggests that due to the high velocity, the spray in this study corresponds to the second wind-induced regime. The stable spray under the effect of cavitation in this study is instrumental in the consistent use for the biological samples. On the other hand, the increase in the velocity of the working fluid leads to an increase in the

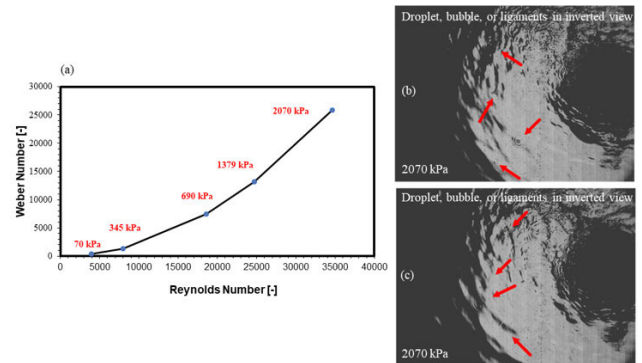


FIGURE 2. a) Reynolds number with respect to Weber number at different back pressures for water as the working fluid, b and c) the inverted view of the spray to emphasize on the presence of the bubbles, droplets, and liquid ligaments.

TABLE 1. Thermophysical properties of DI water and PBS.

	DI Water	PBS
Density ( $\rho$ ) [kg/m <sup>3</sup> ]	998.2	1060
Surface tension ( $\gamma$ ) [mN/m]	72.2	69.5
Saturated vapor pressure ( $P_{vap}$ ) [kPa]	2.33	2.27
Dynamic viscosity ( $\mu$ ) [Pa.s]	$8.9 \times 10^{-4}$	$9.04 \times 10^{-4}$
Kinematic Viscosity ( $\nu$ ) [m <sup>2</sup> /s]	$8.91 \times 10^{-7}$	$8.52 \times 10^{-7}$

turbulence intensity, which could be manifested by analyzing the Reynolds number at different back pressures. For this purpose, the Reynolds number is plotted against Weber number in Figure 2.

According to our observation, the Weber number increases with Reynolds number. Consequently, a more turbulent spray leads to a more tendency of the jet to break-up. Moreover, the ligament generation in the spray can be observed at high pressures (such as 2070 kPa). The inverted view of the spray is included in Figure 2- b, c. As indicated, the droplet, cavitation bubble, and ligaments hit the surface. These generated particles from the spray are responsible for the observations on cell lines, which will be considered in the next section. The working fluid for the biological section in the present study is PBS. Therefore, it is vital to compare the results of the fluid regime of PBS with those obtained when using water. The thermophysical properties of the working fluids are the main difference between the sprays with either water or PBS. Table 1 shows the thermophysical properties of both water and PBS [10].

Ohnesorge number, which presents the effect of kinematic viscosity on the jet flow behavior, is 0.00655 for the case of water in the present geometry, whereas this value is 0.00658 for the case of PBS. Accordingly, the kinematic viscosities are close to each other for both working fluids so that their Ohnesorge numbers are also similar. The obtained kinematic viscosity values suggest that a change in the working

fluid from water to PBS has a minor role in changing the spray behavior. However, the only advantage of the use of PBS is preserving the viability of the cells.

In the following section, cavitating flows are targeted to the immobilized cancer cell lines on the surface. The morphological disruptions caused by the exposure of the cavitating flow are investigated using the SEM technique. The impact of cavitating flows on disruption of the cells is discussed. The mechanical properties of the cancer cell lines and the impact pressure due to cavitating flows are compared, and the disruption of the cells is linked with the bubble size.

In the following section, cavitating flows are targeted to the immobilized cancer cells lines on the surface. The morphological disruptions caused by the exposure of the cavitating flow are investigated using the SEM technique. The impact of cavitating flows on disruption of the cells is discussed. The mechanical properties of the cancer cells lines and the impact pressure due to cavitating flows are compared, and the disruption of the cells is linked with the bubble size.

### **B. MORPHOLOGICAL CHANGE OF IMMOBILIZED CANCER CELLS ON A CHIP**

In general, the morphological changes of the cancer cell structure and surface are distinguishable by cell hypertrophy phenomenon due to irregular shape and massive nucleus because of the acceleration of the cell genomic activity and proliferation. The frequent vacuoles and large nucleus occupy most of the cell mass and form the compact cytoplasm with a noticeable accumulation of ribosomes and polysome, whose shape is in a cluster formation [33]. Degranulation and defragmentation within the cells occur due to the intervention of mitochondria and granular endoplasmic reticulum with other organelles, which eventually changes the cell morphology enormously. The enhancement of nuclear membrane pores leads to the formation of the surface granulated structure. The significant amount of the intermediate filaments and microfilaments -knot shapes- are massively raised to elevate the rate of metastasizing in all the directions [34]. Normal cells contain a plasma membrane “finger-like” projections, which are generated from bundles of actin filaments, known as Filopodia. The cell filopodia play a significant role in various cellular processes such as cell adhesion, cell-cell communication, and migrations. In cancer cells, ‘integrin proteins’ accumulation in the tip of the filopodia occur due to over production as a result of high metabolism rate and therefore generates higher density structures of filopodia and intensifies motility and adhesions in cancer cells [26]. Hydrodynamic cavitation targeting tumor cell filopodia, which play as cellular pillars, could be a promising technique for the physical elimination of the cell’s structural integrity.

Previous studies show that hydrodynamic cavitation killed cells through the activation of apoptosis, a classical form of programmed cell death [24]. Although we could obtain a fraction of the cells damaged after cavitation experiments, we wondered whether the morphological damage caused by hydrodynamic cavitation in different cancer cells could

lead to the activation of programmed cell death pathways. The morphological characteristics of apoptosis include the rounding and detachment of cells, chromatin condensation, nuclear fragmentation, and apoptotic body formation. At a molecular level, the activation of cell death-related hydro-lases called caspases is defined as one of the hallmarks of apoptosis [29].

In this study, we investigated the effect of cavitating flows on various cell lines including Human Colorectal Carcinoma (HCT-116), Breast Adenocarcinoma (MDA-MB-231), and Ovarian Adenocarcinoma (ONCO-DG-1) cell lines. Each cell line was initially grown on silica / glass surfaces under controlled standard conditions and brought to experimental setup right before the test and returned to the relevant medium after the exposure to assure that ambient conditions did not affect the morphology of the cells. The samples were exposed to cavitating flows for a short time of 3 seconds to make sure that the cancer cells were preserved on the surface after the experiment. To investigate the impact of spray-on cancer cells and normal cells, each cell line was exposed to cavitation using PBS as the working fluid. PBS was used to preserve the viability of the cells. Two samples with the same properties were prepared and harvested for each cell line. Thus, the conditions of the cells before and after the spray exposure were compared. Hydrodynamic cavitation was applied for durations of 3 seconds with the back pressures of 1720 kPa and 3450 kPa. This pressure threshold was chosen to maintain the second wind-induced spray regime according to the flow characterization in the previous section. For pressures lower than 1720 kPa, the cells were not affected significantly, while the cells were completely detached from the silicon surface for pressures higher than 3450 kPa. Once the cell-coated surfaces were exposed to cavitation, they were washed with PBS and subsequently prepared for SEM images. Thus, the effects before and after the experiment could be assessed and compared for ONCO-DG-1, MDA-MB-231 and HCT-116 cancer cell lines.

Figures 4-7 display the SEM images of the cancer cells after the exposure of cavitation. As can be observed, the effect of cavitation on the cancer cells is insignificant at the pressure of 1720 kPa (See Supplementary Information 1, Figure S1). However, the impact created by cavitation bubbles on the cell structure can be clearly observed beyond the pressure of 2070 kPa. When the effect of cavitation is considered for the pressures ranging from 2070 to 3450 kPa, the cells receive damage in different levels, while cell filopodia become detached from the silicon wafer surface beyond the pressure of 3450 kPa. Figure 7 shows the SEM image of cancer cells at 3540 kPa. It can be clearly observed that when pressure is 3450 kPa, the cell membrane and filopodia structure break down. A morphological demolition occurs on the surfaces of ONCO-DG1 cell lines when exposed to the cavitation at pressures between 2070 and 2760 kPa. Figures 4A and 4B exhibits the trace of cavitation bubble effects on the cell surface at 2070 kPa. Nevertheless, when the pressure is raised to 2760 kPa, despite of complete demolition of the filopodia

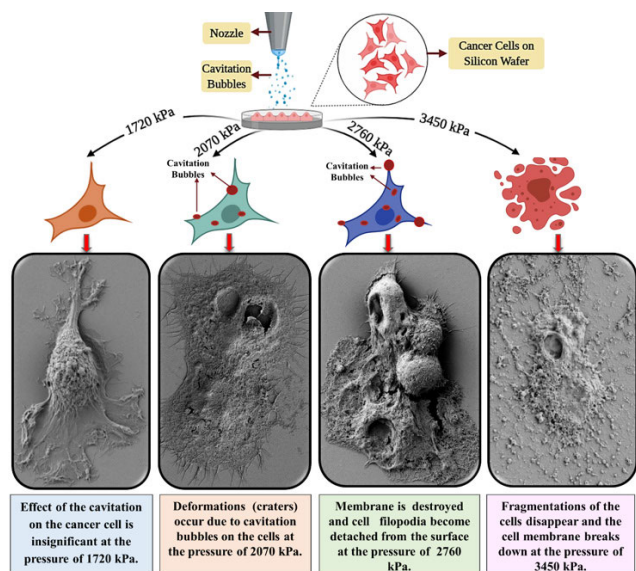


**FIGURE 3.** Morphological deformation modes on the surface of ONCO-DG-1 (Ovarian Adenocarcinoma) cancer cells exposed to cavitation (carpet bombardment) are shown. The effect of cavitation on the cancer cell is insignificant at the pressure of 1720 kPa. Bubble deformations (craters) are observed on the cell membrane at the pressure of 2070 kPa. At 2760 kPa, the membrane is destroyed and cell filopodia is detached. At 3450 kPa, cell fragmentations completely disappear.

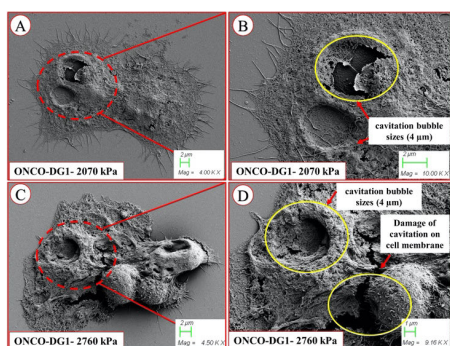


**FIGURE 4.** Effect of cavitation at different pressure values (2070 and 2760 kPa) on ovarian cancer cell shown in A and C. The deformation of the cell membrane caused by cavitation is shown. Subfigures B and D show that the craters formed upon the exposure to cavitation have similar sizes compared to the cavitation bubble sizes (4 μm). Deformations occur in the cell membrane as can be seen in D.

structure, the cells remain attached to the surface as can be seen in Figures 4C and 4D.

As can be seen in Figures 4-7, the diameter of the craters on the cancer cells in SEM images is approximately 4 μm. Our previous studies [4] show that the size of the collapsing bubbles in cavitating flows in a microfluidic device with similar channel dimensions was around 3.5 μm (See Supplementary Information S2). As a result, it can be concluded that the collapse of cavitating bubbles plays a significant role in the disruption of immobilized cancer cells.

#### IV. DISCUSSION

Five modes of flow regime in the liquid jet was introduced by Zhan *et al.* [1] namely, dripping mode, Rayleigh regime, first wind-induced regime, second wind-induced regime, and atomization. The break-up length varies with an increase in

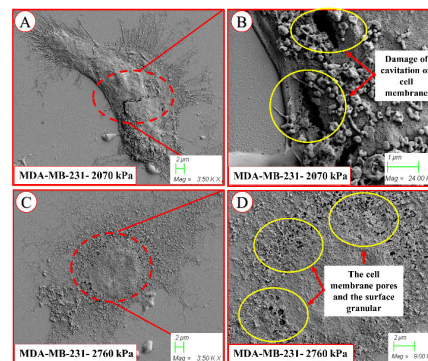


**FIGURE 5.** Effect of cavitation at different pressures on a breast cancer cell shown in A and C. Fragmentations of the cell are destroyed using cavitation as can be seen in A and B. Subfigures C and D show the cellular membrane pores are enlarged, and the surface granular structure is disrupted.

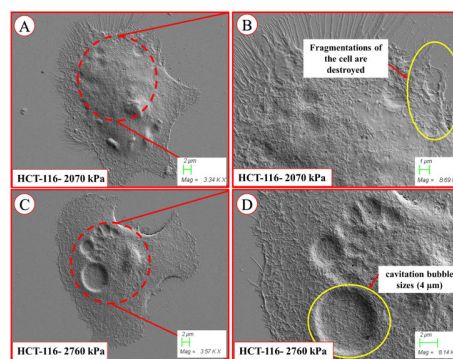


**FIGURE 6.** Effect of cavitation at different pressures on a Colon cancer cell shown in A and C. While cell fragmentations remain on the colon cancer cell surface at 2070 kPa, as can be seen from D, at 2760 kPa pressure, the fragmentations of the cell disappear, and deformations occur in the bubble sizes formed on the surface. The craters formed upon the exposure to cavitation has similar sizes compared to the cavitation bubble size (4 μm).

fluid velocity in different regimes. In dripping mode, the jet velocity is significantly low, while the jet is very unstable in atomization mode. These modes are not of interest of the present study. In the Rayleigh regime and second wind-induced regimes, the break-up length increases with the velocity, while the first wind-induced regime shows the opposite behavior, since this regime is considered as the transition flow regime in the literature. It is worth noting that in the Dripping regime, the size of the generated droplets is large, and they have a low kinetic energy as they are generated by the gravity. In addition, in the first wind induced regime, although the droplets are at the same order of magnitude as the nozzle diameter, they are relatively larger. The size of the cancer cells in the next section are significantly lower than the nozzle diameter (256 μm). In the atomization regime, the kinetic energy of the droplets is too high to be used for the biological purpose of this study. In other words, they can wash the immobilized cancer cells on the surface in the biological study. As a result, second wind induced breakup regime is preferred in this study. The results obtained during the experiments and in the SEM images show that

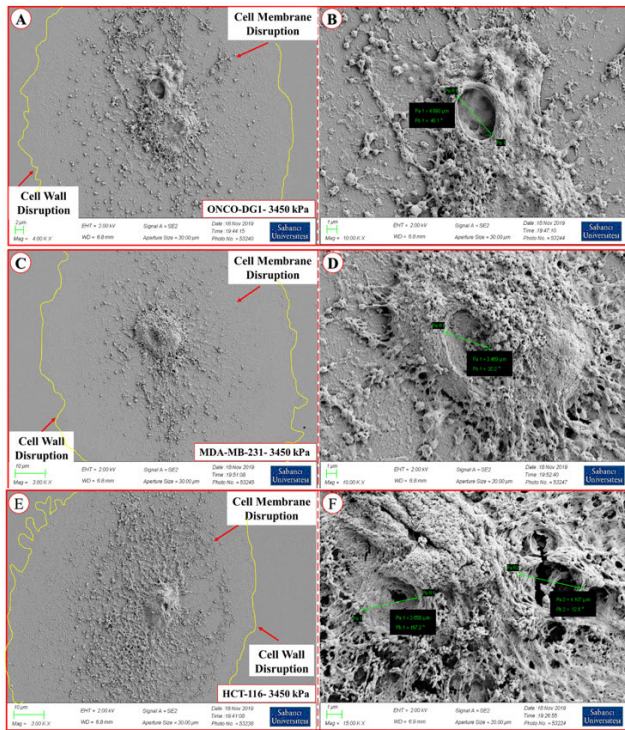


**FIGURE 7.** Effect of cavitation at 3450 pressure on cancer cells. Subfigures A and B show the effect of cavitation on the ONCO-DG-1 (Ovarian Adenocarcinoma) cell line. Subfigures C and D show the effect of cavitation on the MDA-MB-231 (Breast Adenocarcinoma) cell line. Subfigures E and D show the effect of cavitation on the HCT-116 (Human Colorectal Carcinoma) cell line. As can be seen, at 3450 kPa, the fragmentations of the cancer cells disappear completely. It can be clearly observed that the cell membrane breaks down.

the hydrodynamic cavitation exposure on the cancer cell disrupts the morphology of the cancer cells in the pressure range between 2070 kPa and 2760 kPa. The hydrodynamic cavitation causes absolute demolition of the cell structure by rupturing cells and consequently vacuoles membranes and leads to the explosion of its contents. The SEM images exhibit single cancer cells affected by cavitation as well as ‘erupted volcano, which is formed upon the explosion erosion of cytoplasmic and extensive vacuole contents and impaired nucleic membrane. Thus, the deformation of the single-cell can be achieved with hydrodynamic cavitation.

The impact pressure of the cavitating bubble collapse could be compared with the mechanical properties of the cancer cells to elaborate more on the effect of bubble collapse on the deformation of the cancer cells. The impact pressure of the cavitating flow could be approximated as [30]:

$$P_{imp} = \frac{\rho_l c_l v_{jet}}{1 + (\rho_l c_l / \rho_c c_c)} \quad (4)$$

where  $l$  index stands for PBS and  $c$  stands for cells. Having the sound velocity ( $c$ ) in both the cells and PBS, the impact pressure of cavitating flow on the cancer cells could be estimated.  $V_{jet}$  in this equation is the velocity of the fluid jet from the nozzle. The sound velocity and density of breast cancer cells are reported as 987 kg/m<sup>3</sup> and 1580 m/s, respectively [31]. On the other hand, the density and sound velocity

**TABLE 2.** Deformations corresponding to different pressures (including the modes of insignificant damage, craters due to bubbles, membrane damage, cell disintegration) for each cell type. From this table, it is evident that the various modes are depending on the cancer cell type.

Cell Type	1720 kPa	2070 kPa	2760 kPa	3450 kPa
ONCO-DG-1				
MDA-MB-231				
HCT-116				

in PBS are reported as 1060 kg/m<sup>3</sup> and 1505 m/s, respectively [32]. As a result, the impact pressure of cavitating flow with PBS could be calculated as 954 GPa whereas the Young’s modulus of different cancer cells is several orders of magnitude less than the impact pressure. The reported Young’s modulus of the cancer cells ranges from 0.1 kPa to a maximum of 7.41 kPa [33], [34]. This comparison could strongly prove that the amount of energy released as a result of the cavitating bubble collapse results in the disruption of cancer cells.

In the light of the experimental results, the deformation on the cancer cell could be compared to each other. In our study, cancer cells (as single-cell) were exposed to cavitating flows at pressures of 1720, 2070, 2760 and 3450 kPa pressure. Figures 4-7 display the SEM images of ONCO DG-1, MDA-MB-231, and HCT-116 cells after cavitation experiments. While all cancer cells were tested under the same experimental conditions and pressure range, it could be well observed that the ONCO-DG-1 cell deformed more than the HCT-116 cell, while the deformation in the MDA-MB-231 cell was more compared to the others.

Table 2 summarizes the deformation modes for each cell line. As can be seen from Table 2, the effect of cavitation on the cancer cells is insignificant at the pressure of 1720 kPa. The cells are still attached to the silicon wafer surface at the pressure of 1720 kPa. At 2070 kPa pressure, deformations (craters) occur due to cavitation on the ONCO-DG-1 cell, while membrane fracture can be observed for the MDA-MB-231 cell. Small scale superficial damage occurs for the HCT-116 cell at this pressure. At the pressure of 2760 kPa, cracks and craters of bubble size are visible for the ONCO-DG-1 cell. The membrane is almost completely disrupted for the MDA-MB-231 cell. line Craters formed upon the exposure to cavitation have similar sizes compared to the cavitation bubble sizes (4 μm) on the HCT-116 cell at the pressure of 2760 kPa. All the cell lines

manifested some degree of cellular disruption and deformation for pressure beyond 1720 kPa. According to our SEM images, the cell disruption on ONCO-DG-1 cell lines at the pressures of 2070 and 2760 kPa is much more cavernous compared to the cell line HCT-116 exposed to the same pressure. Fragmentations disappear and cell membrane rupture is evident at the pressure of 3540 kPa for all the cell lines. Thus, based on the differences in local deformation of single cells or small samples/tissues upon carpet bombardment with hydrodynamic cavitation, the presented platform could serve as an effective diagnostic tool.

## V. CONCLUSION

This study presents the effect of hydrodynamic cavitation on immobilized single cancer cells. The spray structure was captured using a high-speed camera. The cavitating flow images were processed using an image processing software at different distances from the tip of the nozzle. The Reynolds, Weber, and Ohnesorge numbers were observed at different back pressures, and the flow structures were compared to assess the flow regimes. The flow regime in all the experiments corresponded to the second wind-induced regime. In the biological part of this study, various cancer cell lines were cultured on a silicon wafer, and they were exposed to cavitation at different pressures. The physical changes in cell morphology as a result of the bombardment with hydrodynamic cavitation bubbles were assessed. As expected, the cavitation bubble collapse demolishes exposed cancer cells. The size of craters on the cell surface formed upon cavitation exposure was close to the size of the cavitation bubble. Based on the promising findings, our study proposes a promising method in cancer treatment with cavitating bubble collapse, where microbubbles could be precisely controlled and directed to the desired locations for both in-vitro and in-vivo applications, as well as the characterization of the biophysical properties of cancer cells. The local differences in deformation of exposed cells/small samples upon hydrodynamic cavitation exposure could be a valuable diagnostic tool for cancer diagnosis.

This method does not involve any expensive biomaterials (such as biomarkers, antibodies) as well as modification/functionalization of the surfaces for any detection. No electronic circuit or equipment (such as deposition of resistance) is needed in the platform. In addition, it does not require any agent (such as quantum dots) for visualization. The process lasts for short time (only few seconds) compared to the other methods. The exposed cells or tissues could be examined upon exposure to cavitating flows, and based on the differences in modes of generated damage/deformation on the cell or tissues, diagnosis could be accomplished. As a result, the proposed approach has the advantages of label-free approach, simple structure and low cost and is a substantial alternative for the existing tools. The proposed method relies on the samples (such as isolated cells or tumor tissues) to be collected from the patients. Thus, the collection of samples is one of the limitations. The other limitation is the development of a method for attaching the sample to the surface

of the platform. This method will vary from sample (cell) to sample (tissue). Since the platform is compact, a small sample size will be sufficient for the platform. In addition, once a suitable recipe is developed just as in this study, it can be repeated for mass production of the platforms.

The overall contribution of the present article to the body of knowledge can be summarized as:

- Introduction of a simple, innovative and promising technique for the potential use in cancer diagnosis
- Introduction of a label-free and low-cost method
- Applicability to tissue samples

In spite of the mentioned advantages of the proposed approach, the system is constrained with the upstream pressure. In other words, when the cells are weakly attached to the surface, a high upstream pressure would lead to their separation from the platform. However, there are effective methods to attach the cells on the surface more strongly, which will be exploited as future work.

## ACKNOWLEDGMENT

(*Moein Talebian Gevari and Gizem Aydemir are co-first authors.*) The authors would like to gratefully appreciate the Equipment utilization support from the Sabanci University Nanotechnology Research and Applications Center (SUNUM).

## REFERENCES

- [1] R. E. Sonntag, C. Borgnakke, G. J. van Wylen, and S. van Wyk, *Fundamentals of Thermodynamics*, vol. 6. New York, NY, USA: Wiley, 1998.
- [2] D. J. Flannigan and K. S. Suslick, "Plasma formation and temperature measurement during single-bubble cavitation," *Nature*, vol. 434, no. 7029, p. 52, 2005.
- [3] M. T. Gevari, A. H. Shafaghi, L. G. Villanueva, M. Ghorbani, and A. Koşar, "Engineered lateral roughness element implementation and working fluid alteration to intensify hydrodynamic cavitating flows on a chip for energy harvesting," *Micromachines*, vol. 11, no. 1, p. 49, Dec. 2019, doi: [10.3390/M111010049](https://doi.org/10.3390/M111010049).
- [4] M. Ghorbani, A. S. Aghdam, M. T. Gevari, A. Koşar, F. Ç. Cebeci, D. Grishenkov, and A. J. Svagan, "Facile hydrodynamic cavitation ON CHIP via cellulose nanofibers stabilized perfluorodroplets inside layer-by-layer assembled SLIPS surfaces," *Chem. Eng. J.*, vol. 382, Feb. 2020, Art. no. 122809.
- [5] M. Ghorbani, H. Chen, L. G. Villanueva, D. Grishenkov, and A. Koşar, "Intensifying cavitating flows in microfluidic devices with poly(vinyl alcohol) (PVA) microbubbles," *Phys. Fluids*, vol. 30, no. 10, Oct. 2018, Art. no. 102001, doi: [10.1063/1.5051606](https://doi.org/10.1063/1.5051606).
- [6] M. Dular, T. Griessler-Bulc, I. Gutierrez-Aguirre, E. Heath, T. Kosjek, A. K. Klemencic, M. Oder, M. Petkovšek, N. Racki, M. Ravnikar, and A. Šarc, "Use of hydrodynamic cavitation in (waste) water treatment," *Ultrason. Sonochem.*, vol. 29, pp. 577–588, Mar. 2016.
- [7] V. Starchevskyy, N. Bernatska, I. Typilo, and I. Khomyshyn, "The effectiveness of food industry wastewater treatment by means of different kinds of cavitation generators," *Chem. Chem. Technol.*, vol. 11, no. 3, pp. 358–364, Aug. 2017.
- [8] M. Ghorbani, A. Mohammadi, A. R. Motezakker, L. G. Villanueva, Y. Leblebici, and A. Koşar, "Energy harvesting in microscale with cavitating flows," *ACS Omega*, vol. 2, no. 10, pp. 6870–6877, Oct. 2017.
- [9] M. T. Gevari, M. Ghorbani, A. J. Svagan, D. Grishenkov, and A. Kosar, "Energy harvesting with micro scale hydrodynamic cavitation-thermoelectric generation coupling," *AIP Adv.*, vol. 9, no. 10, Oct. 2019, Art. no. 105012.
- [10] M. T. Gevari, A. Parlar, M. Torabfam, A. Koşar, M. Yüce, and M. Ghorbani, "Influence of fluid properties on intensity of hydrodynamic cavitation and deactivation of salmonella typhimurium," *Processes*, vol. 8, no. 3, p. 326, Mar. 2020, doi: [10.3390/PR8030326](https://doi.org/10.3390/PR8030326).

- [11] M. Ghorbani, C. Sozer, G. Alcan, M. Unel, S. Ekici, H. Uvet, and A. Koşar, "Biomedical device prototype based on small scale hydrodynamic cavitation," *AIP Adv.*, vol. 8, no. 3, Mar. 2018, Art. no. 035108.
- [12] M. T. Gevari, T. Abbasiasl, S. Niazi, M. Ghorbani, and A. Koşar, "Direct and indirect thermal applications of hydrodynamic and acoustic cavitation: A review," *Appl. Thermal Eng.*, vol. 171, May 2020, Art. no. 115065.
- [13] J. A. Rooney, "Hemolysis near an ultrasonically pulsating gas bubble," *Science*, vol. 169, no. 3948, pp. 869–871, Aug. 1970.
- [14] M. W. Miller, D. L. Miller, and A. A. Brayman, "A review of *in vitro* bioeffects of inertial ultrasonic cavitation from a mechanistic perspective," *Ultrasound Med. Biol.*, vol. 22, no. 9, pp. 1131–1154, Jan. 1996.
- [15] S. Mitragotri, "Healing sound: The use of ultrasound in drug delivery and other therapeutic applications," *Nature Rev. Drug Discovery*, vol. 4, no. 3, pp. 255–260, Mar. 2005.
- [16] K. Hynynen, N. McDannold, N. A. Sheikov, F. A. Jolesz, and N. Vykhodtseva, "Local and reversible blood–brain barrier disruption by noninvasive focused ultrasound at frequencies suitable for trans-skull sonications," *NeuroImage*, vol. 24, no. 1, pp. 12–20, Jan. 2005.
- [17] P. Zhong, "Shock wave lithotripsy," in *Bubble Dynamics and Shock Waves*. Berlin, Germany: Springer, 2013, pp. 291–338.
- [18] Z. Xu, T. L. Hall, J. B. Fowlkes, and C. A. Cain, "Effects of acoustic parameters on bubble cloud dynamics in ultrasound tissue erosion (histotripsy)," *J. Acoust. Soc. Amer.*, vol. 122, no. 1, pp. 229–236, Jul. 2007.
- [19] Z. Fan, H. Liu, M. Mayer, and C. X. Deng, "Spatiotemporally controlled single cell sonoporation," *Proc. Nat. Acad. Sci. USA*, vol. 109, no. 41, pp. 16486–16491, Oct. 2012.
- [20] A. Vogel, J. Noack, G. Hüttman, and G. Paltauf, "Mechanisms of femtosecond laser nanosurgery of cells and tissues," *Appl. Phys. B, Lasers Opt.*, vol. 81, no. 8, pp. 1015–1047, Dec. 2005.
- [21] P. A. Quinto-Su, X. H. Huang, S. R. Gonzalez-Avila, T. Wu, and C. D. Ohl, "Manipulation and microrheology of carbon nanotubes with laser-induced cavitation bubbles," *Phys. Rev. Lett.*, vol. 104, no. 1, Jan. 2010, Art. no. 014501.
- [22] F. Li, C. U. Chan, and C. D. Ohl, "Yield strength of human erythrocyte membranes to impulsive stretching," *Biophys. J.*, vol. 105, no. 4, pp. 872–879, Aug. 2013.
- [23] J. Lautz, G. Sankin, F. Yuan, and P. Zhong, "Displacement of particles in microfluidics by laser-generated tandem bubbles," *Appl. Phys. Lett.*, vol. 97, no. 18, Nov. 2010, Art. no. 183701.
- [24] Z. Itah, O. Oral, O. Y. Perk, M. Sesen, E. Demir, S. Erbil, A. I. Dogan-Ekici, S. Ekici, A. Kosar, and D. Gozuacik, "Hydrodynamic cavitation kills prostate cells and ablates benign prostatic hyperplasia tissue," *Experim. Biol. Med.*, vol. 238, no. 11, pp. 1242–1250, Nov. 2013.
- [25] H. Ashush, R. LA, M. Blass, M. Barda-Saad, D. Azimov, J. Radnay, D. Zipori, and U. Rosenschein, "Apoptosis induction of human myeloid leukemic cells by ultrasound exposure," *Cancer Res.*, vol. 60, no. 4, pp. 1014–1020, 2000.
- [26] A. Arjonen, R. Kaukonen, and J. Ivaska, "Filopodia and adhesion in cancer cell motility," *Cell Adhes. Migration*, vol. 5, no. 5, pp. 421–430, Sep. 2011.
- [27] D. F. Young, B. R. Munson, T. H. Okiishi, and W. W. Huebsch, *A Brief Introduction to Fluid Mechanics*. Hoboken, NJ, USA: Wiley, 2010.
- [28] M. Ghorbani, A. K. Sadaghiani, M. Yidiz, and A. Koşar, "Experimental and numerical investigations on spray structure under the effect of cavitation phenomenon in a microchannel," *J. Mech. Sci. Technol.*, vol. 31, no. 1, pp. 235–247, Jan. 2017.
- [29] G. Kroemer et al., "Classification of cell death: Recommendations of the nomenclature committee on cell death 2009," *Cell Death Differentiation*, vol. 16, no. 1, pp. 3–11, Jan. 2009.
- [30] M. Karimzadehkhoei, M. Ghorbani, M. Sezen, K. Şendur, M. P. Mengüç, Y. Leblebici, and A. Koşar, "Increasing the stability of nanofluids with cavitating flows in micro orifices," *Appl. Phys. Lett.*, vol. 109, no. 10, Sep. 2016, Art. no. 104101.
- [31] E. M. Strohm, G. J. Czarnota, and M. C. Kolios, "Quantitative measurements of apoptotic cell properties using acoustic microscopy," *IEEE Trans. Ultrason., Ferroelectr., Freq. Control*, vol. 57, no. 10, pp. 2293–2304, Oct. 2010.
- [32] J. L. Raymond, K. J. Haworth, K. B. Bader, K. Radhakrishnan, J. K. Griffin, S.-L. Huang, D. D. McPherson, and C. K. Holland, "Broad-band attenuation measurements of phospholipid-shelled ultrasound contrast agents," *Ultrasound Med. Biol.*, vol. 40, no. 2, pp. 410–421, Feb. 2014.
- [33] A. I. Baba and C. Cătoi, "Tumor cell morphology," in *Comparative Oncology*. Bucharest, Romania: The Publishing House of the Romanian Academy, 2007, ch. 3.
- [34] B. Enyedi and P. Niethammer, "Nuclear membrane stretch and its role in mechanotransduction," *Nucleus*, vol. 8, no. 2, pp. 156–161, Mar. 2017.



**MOEIN TALEBIAN GEVARI** received the B.Sc. degree in mechanical engineering from Shahid Beheshti University, Tehran, Iran, in 2018, and the M.Sc. degree in mechatronics from Sabanci University, Istanbul, Turkey, in 2020, with a focus on physics and applications of hydrodynamic cavitation in microfluidic devices. He is currently pursuing the Ph.D. degree in electrical engineering with Uppsala University, Uppsala, Sweden. He dedicated his early research to the numerical and experimental studies in Microfluidics. He is also investigating the design and development of an electrokinetic-based microfluidics biosensor for early-stage lung cancer diagnosis. His research interests include numerical and experimental studies on microfluidic devices with industrial and/or laboratory scale applications.



**GIZEM AYDEMİR** received the B.S. degree in mechatronics engineering from Istanbul Gedik University, in 2017, and the M.Sc. degree in mechatronics engineering from Yildiz Technical University, in 2020, with a focus on micro-robotic system development for the characterization of single-cell mechanical properties in microfluidic devices. She is currently working on the design and implementation of micro-electro-mechanical system (MEMS) sensors for mechanical characterization of muscle disease diagnosis, Institute for Intelligent Systems and Robotics (ISIR), Sorbonne University. Her research interests include the micro-robotics systems, micro-electro-mechanical systems (MEMS), magnetic actuators, lab-on-a-chip devices, and their biomedical applications.



**GHAZALEH GHARIB** received the B.Sc. degree in general biology from the University of Mashhad, Iran, the M.Sc. degree in biotechnology from the Institute of Biochemistry and Biotechnology (IBB), University of the Punjab, Pakistan, and the Ph.D. degree in biotechnology from the School of Biological Sciences (SBS), University of the Punjab, in early 2017. She was awarded Higher Education Commission (HEC) fully funded scholarship to pursue M.Phil. degree leading to Ph.D. degree. She has been working extensively on microbial oxidoreductase enzymes structures, mechanism of actions and their clinical/ industrial applications. She served as a Visiting Faculty for the De'Montmorency College of Dentistry, Lahore, Pakistan, where she received the Excellence in Teaching Award for her outstanding performance. Upon receiving her Ph.D. in 2017, she was appointed as an Assistant Professor with the University of Central Punjab (UCP), Lahore, Pakistan. Subsequently, she was an awarded TUBITAK International Fellowship in 2018 to pursue her Postdoctoral Research on her proposed project based on the clinical application of thermostable enzyme coated nanoparticles at the Sabanci University Nanotechnology Research, and Application Center (SUNUM), Istanbul, Turkey. She is currently a Postdoctoral Research Associate with the Faculty of Engineering and Natural Sciences (FENS), Sabanci University, and SUNUM, where she also works on various multidisciplinary bio-integrated projects, including bioengineering and cancer therapy.





**OZLEM KUTLU** received the B.S. degree from the Department of Biology, Ege University, Izmir, in 2002, and the M.Sc. and Ph.D. degrees from the Department of Material and Life Science, Kumamoto University, Japan, in 2008. From 2009 to 2012, she was a Postdoctoral Fellow in Molecular Biology, Genetics, and Bioengineering Program, Sabanci University, Istanbul. She is currently an Associate Professor and a Research Team Leader with the Sabanci University Nanotechnology Research and Application Center (SUNUM). Her research interest includes molecular regulation of genetic diseases. She focuses on Human Rare (Gaucher, Ichthyosis, and Niemann-Pick) and common Genetic Disease (Alzheimer and Parkinson), Drug/Gene Delivery with Biodegradable Nanoparticles and Biomedical Application of novel Medical Devices.



**MORTEZA GHORBANI** received the Ph.D. degree in micro scale cavitation and its applications from Sabanci University, in 2017. He subsequently undertook Postdoctoral Research work at Sabanci University and the KTH Royal Institute of Technology. In 2019, he moved to the Sabanci University Nanotechnology Research and Application Center, where he became a Principal Investigator on microfluidics and cavitation. He currently heads the Cavitation and Interfaces Research Group. He is also serving as an Editor for the *Biomed Research International Journal*. He is also a Topic Editor in *Biosensors Journal*. He is also acting as a Researcher with the Medicine Technology and Health System School, KTH Royal Institute of Technology, Sweden.



**HUSEYIN UVET** received the B.S. degree in computer science from Istanbul Kultur University, Istanbul, Turkey, in 2004, and the M.S./Ph.D. degrees from Osaka University Systems Science and Applied Informatics, Osaka, Japan, in 2007 and 2010, respectively, with the focus on micro/nano-robotics and lab-on-a-chip systems. He is currently an Assistant Professor with Department of Mechatronics Engineer, Yildiz Technical University. His research interests include micro/nano-robotics, lab-on-a-chip devices, biomedical robotics, and micro-nano air vehicles. He is an Expert System Innovation Engineer with a diverse ability in mechatronics device engineering and assembly process automation. He received numerous prizes and awards from prestigious international and national competitions, conferences.



**ALI KOŞAR** received the B.S. degree in mechanical engineering from Boğaziçi (Bosphorus) University, Istanbul, and the master's degree from the Department of Mechanical Engineering, Rensselaer Polytechnic Institute. After completing his M.S. and Ph.D. degrees, he worked with the Rensselaer Polytechnic Institute, as an Adjunct Faculty Member. He joined the Mechatronics Engineering Program at Sabanci University, in Fall 2007. He is currently a Professor with Sabanci University and the Co-Director of the Center of Excellence for Functional Surfaces and Interfaces for Nano diagnostics (EFSUN). His research interests include heat and fluid flow in micro/nano domains and boiling and cavitation in micro/nano scale. The results of his research have already generated more than 130 journal research articles in prestigious journals. He received national and international awards, such as the Middle East Technical University (METU) Prof. Mustafa N. Parlar Foundation Technology Award in 2017, the Sedat Simavi Foundation Natural Sciences Award in 2016, the Ten Outstanding Young Persons Turkey Award in Scientific Leadership (TOYP 2015), the American Society of Mechanical Engineers (ASME) International Conference on Nanochannels, Microchannels, and Minichannels (ICNMM) Outstanding Early Career Award, Japan, in 2013, the Kadir Has Outstanding Young Investigator Award, in March 2013, the TUBITAK (The Scientific and Technological Research Council of Turkey) Incentive Award in July 2012, and the Outstanding Young Researcher Award of Turkish Academy of Sciences in 2011.

...